

SINGULARITIES AND THE CONVERGENCE RATE OF A SOLUTION FOR STOKES FLOW IN A CAVITY WITH FREE SURFACES

Fuat GÜRCAN

Department of Mathematics, Faculty of Arts and Sciences, Erciyes University, 38039 Kayseri-TURKEY,
gurcan@erciyes.edu.tr

Abstract : Two-dimensional Stokes flow equation in a rectangular cavity with two free surfaces and two moving lids is considered as a biharmonic boundary value problem which is solved analytically for the streamfunction, ψ , expressed as a series of eigenfunctions. The series solution is shown to converge. In practice, the series must be truncated after N terms, so it is important to assess the number of terms required to achieve a given accuracy in the streamfunction and velocity at any point in different cavities. The accuracy and convergence rate of the eigenfunction series are discussed. Furthermore, we study the influence of the singularities on the corners with respect to the accuracy of the solution. The singularities result in a reduced convergence of the eigenfunctions expansion in a small neighbourhood of the corners.

SERBEST YÜZEYLİ BİR OYUKTAKİ STOKES DENKLEMİNİN ÇÖZÜMÜNÜN SİNGÜLERİTELERİ VE YAKINSAKLIK ORANI

Özet: İki serbest yüzeyle ve iki hareketli kapak arasındaki dikdörtgen bir bölgede, iki boyutlu Stokes denklemi biharmonik sınır değer problemi olarak göz önüne alındı. Bu problem eigen fonksiyonların bir serisi ile analitik olarak çözüldü ve bu çözümün yakınsaklığı gösterildi. Uygulamada, sonsuz bir seri belli bir terimden sonra kesilmesi gerektiğinden. Bu kesmenin, boyutları farklı bölgelerin herhangi bir noktasında akış fonksiyonu ve türevinin yakınsaklık oranına etkisi tartışıldı. Ayrıca köşelerdeki singüler noktaların çözüme etkisi incelendi. Singülerlik, köşelerin küçük komşuluğundaki çözümün yakınsaklık oranını düşürdüğü belirlendi.

Introduction

Although Stokes equations have been investigated for nearly 150 years, analytic solutions have been obtained only for special geometries. For a semi-bounded domain, Smith [1] established an algorithm for solving the biharmonic equation. Smith also established conditions on the edge data sufficient to guarantee the convergence of his analytical solution which is expressed as an infinite series of complex eigenfunctions (Papkovitch-Fadle functions). Smith's solution was then used by Joseph and Sturges [2] to analyse Stokes flow in a rectangular cavity heated from its side. This work, together with that of Joseph [3] revealed that Smith's conditions on the edge data were too restrictive for practical applications and showed that much less restrictive ones suffice to guarantee convergence of Smith's analytical solution.

Joseph and Sturges [4] examined numerically the convergence of an biorthogonal solution of Stokes flow in a single-lid-driven cavity with free solid walls to the boundary conditions. It was found that by taking $n=20$ terms of the biorthogonal series solution the convergence of the streamfunctions and its normal derivatives to the boundary

onditions on the moving lid are given correct to 4 and one decimal place, respectively. Gürcan [5] investigated the truncation error of the infinity series for this problem. It was found that the truncation errors decreases when more terms in the series are taken, as expected. For the same problem Shankar [6] considered an analytic series expansion but used a least squares method to determine the coefficient in the series. He examined the convergence of the least squares solution on the moving lid, especially near to the corner at which there is a singularity. He concluded that both coefficient determination methods are indistinguishable from one another. Stokes Flow in a rectangular cavity with two free surfaces and two moving lids was proposed as a model for the flow in the bead of meniscus roll coater [7-9]. Generally they investigated flow structure by considering the behaviour of streamfunction close to stagnation points.

In this study, the series solution for this problem is considered. The convergence of the series solution is shown by determining the dominant contribution to each term in the series. We also determine the number of terms, n , of the series in order to ensure that the truncation error is acceptably small. The problem of interest exhibits corner singularities due to the inadmissibility of the no-slip hypothesis near the junction between a moving lid and a free surface [10]. The numerical study of flow singularities is very important since they typically increase computational errors [11-13]. A local singular analytical solution of [10] is used to correct the numerical methods in [12-13]. Here we investigate the influence of the singularities on the corners with respect to the accuracy of the series solution.

The Governing Equation and Boundary Conditions

Flow in a double-lid-driven cavity with 2 free surfaces and 2 moving lids, see figure 1, is governed by the biharmonic equation,

$$\nabla^4 \Psi = 0. \quad (1)$$

The analysis is simplified by introducing the following dimensionless variables,

$$u = U/V_2, \quad v = V/V_2, \quad x = X/L, \quad y = Y/L \quad \text{and} \quad \psi = \Psi/V_2 L$$

$$S = V_1/V_2, \quad A = H_0/L$$

where $2L$ is the bead width, V_1 the top lid velocity, V_2 the bottom lid velocity, $S = V_1/V_2$ the speed ratio, $2H_0$ the separation of the lids and $A = 2H_0/L$ the aspect ratio of the cavity.

For the lid-driven cavity with 2 free surfaces we assume that the liquid domain is closed and no liquid crosses the boundaries. This implies that

$$\psi(1, y) = \psi(-1, y) = 0 \quad \text{and} \quad \psi(x, A) = \psi(x, -A) = 0. \quad (2)$$

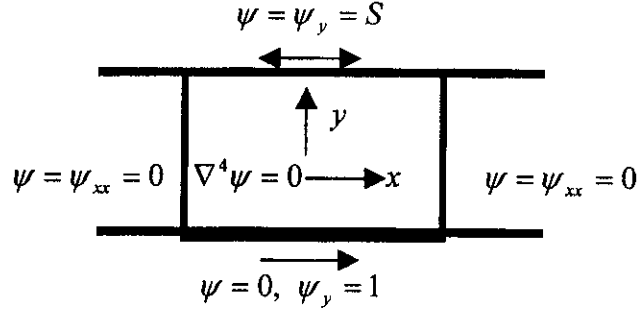


Figure 1: Dimensionless boundary value problem for rectangular cavity with two free surfaces.

Hence relations, $u = \frac{\partial \psi}{\partial y}$ and $v = -\frac{\partial \psi}{\partial x}$, enable the no-slip conditions to be written in terms of derivatives of the streamfunction.

$$\frac{\partial \psi}{\partial y}(x, A) = S, \quad \frac{\partial \psi}{\partial y}(x, -A) = 1. \quad (3)$$

If $\hat{n} = (\pm 1, 0)$, $\hat{t} = (0, \pm 1)$ are unit vectors normal and tangential to the liquid-gas interface respectively, then the equation expressing the equilibrium of this interface [14-p69] is

$$\underline{\underline{\sigma}} \cdot \hat{n} = \underline{\underline{\sigma}}_g \cdot \hat{n} + \frac{T}{R_{curv}} \cdot \hat{n}, \quad (4)$$

where $\underline{\underline{\sigma}}$ and $\underline{\underline{\sigma}}_g$ are the stress tensors for the liquid and gas respectively, T is the surface tension of the liquid, and R_{curv} the radius of curvature of the liquid-gas interface. For a Newtonian liquid the stress tensor is given by

$$\underline{\underline{\sigma}}_{ij} = -P\delta_{ij} + \eta\left(\frac{\partial u_i}{\partial x_j} + \frac{\partial u_j}{\partial x_i}\right), \quad (5)$$

where δ_{ij} is the Kronecker delta symbol. It can be shown, balancing shear stresses, that

$$\eta\left(\frac{\partial u}{\partial y} + \frac{\partial v}{\partial x}\right) = \eta_g\left(\frac{\partial u_g}{\partial y} + \frac{\partial v_g}{\partial x}\right) \quad (6)$$

where the subscript g refers to the gas. However $\eta_g/\eta \ll 1$, so equation (6) reduces to a 'zero-shear stress' condition, namely

$$\frac{\partial u}{\partial y} + \frac{\partial v}{\partial x} = 0 \text{ at } x = \pm 1. \quad (7)$$

Using relations, $u = \frac{\partial \psi}{\partial y}$ and $v = -\frac{\partial \psi}{\partial x}$, this may be written in terms of the streamfunction, giving

$$\frac{\partial^2 \psi}{\partial y^2} - \frac{\partial^2 \psi}{\partial x^2} = 0 \text{ at } x = \pm 1. \quad (8)$$

As a result of boundary condition (2)

$$\frac{\partial \psi}{\partial y} = \frac{\partial^2 \psi}{\partial y^2} = 0 \text{ at } x = \pm 1, \quad (9)$$

and the zero-shear stress condition becomes

$$\frac{\partial^2 \psi}{\partial x^2} = 0 \text{ at } x = \pm 1. \quad (10)$$

General Solution

The boundary value problem, figure 1, can be solved for ψ using 'natural' eigenfunctions of the biharmonic equation which are even functions of x since the flow is symmetric about $x = 0$. In fact $\psi(x, y)$ has the form

$$\psi = \sum_{n=1}^{\infty} \left\{ y(A_n e^{\lambda_n y} + B_n e^{-\lambda_n y}) + C_n e^{\lambda_n y} + D_n e^{-\lambda_n y} \right\} \cos \lambda_n x, \quad (11)$$

where λ_n are eigenvalues and A_n, B_n, C_n, D_n are constant coefficients to be determined from the boundary conditions. The conditions, $\psi = \frac{\partial^2 \psi}{\partial x^2} = 0$ at $x = \pm 1$ are satisfied if $\cos \lambda_n = 0$ for all λ_n , giving the eigenvalues

$$\lambda_n = (n - \frac{1}{2})\pi \text{ for } n = 1, 2, \dots \quad (12)$$

Since the streamfunction $\psi(x, y)$ satisfies the boundary condition (2) on $y = A$ then $\psi(x, y)$ can be written in the form

$$\psi = \sum_{n=1}^{\infty} \psi_n \cos \lambda_n x, \quad (13)$$

where

$$\psi = (y - A)(A_n e^{\lambda_n y} + B_n e^{-\lambda_n y}) - A \frac{A_n e^{-2\lambda_n y} + B_n e^{\lambda_n y} (1 - e^{2\lambda_n(A-y)})}{\sinh 2\lambda_n A}. \quad (14)$$

Since $\frac{\partial \psi}{\partial y}(x, A) = S$ and also $\frac{\partial \psi}{\partial y}(x, -A) = 1$ then using the orthogonality

condition A_n and B_n are obtained

$$A_n = \frac{(-1)^{n+1} \left[\left(e^{\lambda_n A} - \frac{2A\lambda_n}{\sinh 2A\lambda_n} e^{-\lambda_n A} \right) S - \left(e^{-\lambda_n A} - \frac{2A\lambda_n}{\sinh 2A\lambda_n} e^{\lambda_n A} \right) \right]}{\frac{\lambda_n}{\sinh 2A\lambda_n} (\sinh^2 2A\lambda_n - 4A^2 \lambda_n^2)} \quad (15)$$

$$B_n = \frac{(-1)^{n+1} \left[\left(e^{\lambda_n A} - \frac{2A\lambda_n}{\sinh 2A\lambda_n} e^{-\lambda_n A} \right) - S \left(e^{-\lambda_n A} - \frac{2A\lambda_n}{\sinh 2A\lambda_n} e^{\lambda_n A} \right) \right]}{\frac{\lambda_n}{\sinh 2A\lambda_n} (\sinh^2 2A\lambda_n - 4A^2 \lambda_n^2)}. \quad (16)$$

Series Truncation and Convergence

Since, in practice, it is only possible to include a finite number of terms in the series (13), it is necessary to first establish that the series converges and then to determine the number of terms which need to be taken in order to ensure that the series has converged satisfactorily.

The series for ψ

It is possible to investigate the convergence of the series for ψ by determining the dominant contribution to each term in the series for large n . First consider the coefficient A_n which may be rewritten as

$$A_n = \frac{(-1)^{(n+1)} \left[\left(\frac{1}{2} - \frac{e^{-4\lambda_n A}}{2} - 2\lambda_n A e^{-4\lambda_n A} \right) S - \left(\frac{e^{-2\lambda_n A}}{2} - \frac{e^{-6\lambda_n A}}{2} - 2\lambda_n A e^{-2\lambda_n A} \right) \right]}{\frac{\lambda_n e^{\lambda_n A}}{4} - \frac{\lambda_n e^{-3\lambda_n A}}{2} + \frac{\lambda_n e^{-7\lambda_n A}}{4} - 4\lambda_n^3 A e^{-3\lambda_n A}}$$

Extracting the dominant term, we see that for large n ,

$$A_n = (-1)^{(n+1)} \frac{2S}{\lambda_n e^{\lambda_n A}} + l.o.t \quad (17)$$

where 'l.o.t.' indicates lower order terms. Similarly for the coefficient B_n ,

$$B_n = (-1)^{(n+1)} \frac{2}{\lambda_n e^{\lambda_n A}} + l.o.t \quad (18)$$

Substituting expressions (17) and (18) into ψ gives for large n

$$\psi_n = (-1)^{(n+1)} \left[\frac{S(y-A)}{\lambda_n e^{\lambda_n(A-y)}} + \frac{(y+A)}{\lambda_n e^{\lambda_n(A+y)}} \right] + l.o.t, \text{ for } -A < y < A \quad (19)$$

Expression (19) gives the dominant terms in ψ both of which are

$$\psi_n = O((-1)^{(n+1)} \frac{1}{\lambda_n} e^{-k\lambda_n}), \quad k > 0 \quad (20)$$

where either $k = A - y$ or $k = A + y$ for $y \in (-A, A)$. The series $\sum \psi_n$ for $S \in [-1, 1]$ is clearly absolutely convergent and hence the series for ψ converges for $y \in [-A, A]$.

To see how convergence varies for different values of y and A , tables 1 and 2 indicate the accuracy on truncation after n terms of the streamfunction calculated from equation (13) for $A = 0.1$ and $A = 1$ respectively and $S = 2/3$. Table 1, for example, shows that for $A = 0.1$ and $y = A/2$ truncating series (13) after $n = 100$ terms gives an accuracy of 9-10 decimal places whereas for $n = 200$ terms the accuracy is 17 decimal places in ψ . This clearly shows that the accuracy of ψ improves very rapidly as the number of terms in the series (13) is increased. Table 2 shows that for $A = 1$ and $y = A/2$ truncating the series after only $n = 20$ terms gives ψ correct to 10 decimal places. Clearly for large A the convergence is much faster than for lower A values, but it also depends on y , as shown tables 1 and 2.

Table 1: A comparison of the accuracy of the streamfunction calculated by the series (13) after n terms (the accuracy is indicated by the underlined numbers) for $A = 0.1$ at $S = 2/3$. n denotes the number of terms used in the series.

| $S = 2/3$ and $A = 0.1$ | | | | |
|-------------------------|-----|-------------------------|--------------------|--------------------|
| y | n | actual values of ψ | | |
| | | $x = -0.7$ | $x = -0.3$ | $x = 0.0$ |
| $y = A$ | 50 | 0.0 | 0.0 | 0.0 |
| | 100 | 0.0 | 0.0 | 0.0 |
| | 200 | 0.0 | 0.0 | 0.0 |
| $y = A/$ | 50 | -0.021887577212570 | -0.021875137363653 | -0.021874876919845 |
| | 100 | -0.021885248376509 | -0.021874999483326 | -0.021874999976018 |
| | 200 | -0.021885248427780 | -0.021874999510103 | -0.021874999999919 |
| | 300 | -0.021885248427780 | -0.021874999510103 | -0.021874999999919 |
| $y = 0$ | 50 | -0.008352175975982 | -0.008333332130091 | -0.00833333302818 |
| | 100 | -0.008352175913157 | -0.008333332094946 | -0.008333333334355 |
| | 200 | -0.008352175913157 | -0.008333332094946 | -0.008333333334355 |
| | 300 | -0.008352175913157 | -0.008333332094946 | -0.008333333334355 |
| $y = -A/$ | 50 | 0.009365349725042 | 0.009375092392383 | 0.009374917946727 |
| | 100 | 0.009365174276404 | 0.009375000472198 | 0.00937499984145 |
| | 200 | 0.009365174310584 | 0.009375000490049 | 0.009375000000079 |
| | 300 | 0.009365174310584 | 0.009375000490049 | 0.009375000000079 |

Table 2: A comparison of the accuracy of the streamfunction given by the series (13) after n terms for $A = 1.00$ at $S = 2/3$.

| $S = 2/3$ and $A = 1.0$ | | | | |
|-------------------------|-----|-------------------------|--------------------|--------------------|
| y | n | actual values of ψ | | |
| | | $x = -0.7$ | $x = -0.3$ | $x = 0.0$ |
| $y = A$ | 20 | 0.0 | 0.0 | 0.0 |
| | 50 | 0.0 | 0.0 | 0.0 |
| | 100 | 0.0 | 0.0 | 0.0 |
| $y = A/$ | 20 | -0.12198463011580 | -0.19330687552501 | -0.20444704539851 |
| | 50 | -0.12198463012672 | -0.19330687554985 | -0.20444704539602 |
| | 100 | -0.12198463012672 | -0.19330687554985 | -0.20444704539602 |
| | 200 | -0.12198463012672 | -0.19330687554985 | -0.20444704539602 |
| $y = 0$ | 20 | -0.031460348869680 | -0.059018667895093 | -0.065249136291313 |
| | 50 | -0.031460348869680 | -0.059018667895093 | -0.065249136291313 |
| | 100 | -0.031460348869680 | -0.059018667895093 | -0.065249136291313 |
| | 200 | -0.031460348869680 | -0.059018667895093 | -0.065249136291313 |
| $y = -A/$ | 20 | 0.063269110456510 | 0.094031267337532 | 0.097425348491845 |
| | 50 | 0.063269110454900 | 0.094031267339420 | 0.097425348492717 |
| | 100 | 0.063269110454900 | 0.094031267339420 | 0.097425348492717 |
| | 200 | 0.063269110454900 | 0.094031267339420 | 0.097425348492717 |

The series for $\frac{\partial \psi}{\partial y}$

Similarly, substituting expressions (17) and (18) into $\frac{\partial \psi}{\partial y}$ gives for large n

$$\frac{\partial \psi_n}{\partial y} = (-1)^{(n+1)} \left[\frac{S \left(\frac{1}{\lambda_n} + (y-A) \right)}{e^{\lambda_n(A-y)}} + \frac{\frac{1}{\lambda_n} - (y+A)}{e^{\lambda_n(A+y)}} \right] + l.o.t \quad (21)$$

For $y \in (-A, A)$

$$\frac{\partial \psi_n}{\partial y} = O((-1)^{(n+1)} e^{k\lambda_n}) \quad \text{where } k > 0 \quad (22)$$

and so the series $\sum \frac{\partial \psi_n}{\partial y}$ is absolutely convergent and hence the series for $\frac{\partial \psi}{\partial y}$ converges for $y \in (-A, A)$.

To see how convergence varies for different values of y and A , table 3 indicates the accuracy of the truncated for $\frac{\partial \psi}{\partial y}$ for various aspect ratios, speed ratios and positions within the cavity. For $A = 0.1$, $S = -1/2$ at $y = -A/2$ truncating $\frac{\partial \psi}{\partial y}$ after 100 terms gives 8 decimal place accuracy and for $n = 200$ sixteen decimal places, see table 3.

This table shows also that for $A = 1$, $S = -1$ and at the same location $y = -A/2$ with only 20 terms, $\frac{\partial \psi}{\partial y}$ shows an accuracy of 14 decimal places. Results clearly show that the convergence of the series for $\frac{\partial \psi}{\partial y}$ depends on y and A . In general for large A the convergence is much faster than for small A but that the convergence decreases as the lids are approached.

On The Lids

The coefficients A_n, B_n are chosen so that the lid velocity boundary conditions are approximated by Fourier series. Hence on the top lid

$$\frac{\partial \psi}{\partial y} = \sum ((-1)^{(n+1)} \frac{S \cos \lambda_n x}{\lambda_n}) \quad (23)$$

and on the bottom lid

$$\frac{\partial \psi}{\partial y} = \sum ((-1)^{(n+1)} \frac{\cos \lambda_n x}{\lambda_n}). \quad (24)$$

Since these series satisfy the 'Dirichlet' conditions for Fourier series convergence they converge to the boundary conditions on the lids everywhere except close to the corners.

Corner Singularities

It can be seen that this problem contains singularities at all corners formed at the junction between a moving lid and a free surfaces. We computed the singular behaviour near the upper-left corner with the procedure described by Moffatt [10] to compare the present results. In this procedure a local solution is computed for the biharmonic equation in plane co-ordinates (r, θ) of the form

$$\Psi = \sum_p r^p f_p(\theta). \quad (25)$$

The boundary value problem to be solved in the corner region has boundary conditions,

$$\Psi = 0, \quad \frac{1}{r} \frac{\partial \Psi}{\partial \theta} = S \quad \text{at } \theta = 0,$$

$$\Psi = 0, \quad \frac{1}{r} \frac{\partial \Psi}{\partial \theta} = 0 \quad \text{at } \theta = \frac{-\pi}{2}.$$

The lowest order solution is $\Psi_1 = r f_1(\theta)$ given by

$$\Psi_1 = \frac{r}{\pi^2 - 4} (4\theta \cos \theta + 2\pi\theta \sin \theta - \pi^2 \sin \theta).$$

The lower order describes the asymptotic behaviour at the corners. The convergence of the coefficients of series (25) shows the same behaviour as we found in our computations whereas the convergence of the derivative of streamfunction (13) is decreased near the corners. However, as the number of terms, n , used in the series $\frac{\partial \Psi}{\partial y}$ is increased, even the convergence in these regions improves. For example, for any value of A , $\frac{\partial \Psi}{\partial y}$ is correct to 2 decimal places when $n = 100$ terms whereas when $n=200$ terms 3-4 decimal places, see table 3.

Table 3. A comparison of the accuracy of the horizontal component of liquid velocity given by the series evaluated after n terms for $A = 0.1$ at $S = -1/2$ and 0 .

| $S = -1/2$ and $A = 0.1$ | | | | |
|--------------------------|-----|-------------------------|-------------------|-------------------|
| y | n | actual values of ψ | | |
| | | $x = -0.7$ | $x = -0.3$ | $x = 0.0$ |
| $y = A$ | 50 | -0.507 | -0.503 | -0.496 |
| | 100 | -0.496 | -0.498 | -0.498 |
| | 200 | -0.498 | -0.499 | -0.499 |
| $y = A/2$ | 50 | 0.34504269983902 | 0.34373097945617 | 0.34376688894477 |
| | 100 | 0.34505909029467 | 0.34374991319534 | 0.34375000713707 |
| | 200 | 0.34505907515618 | 0.34374991531351 | 0.34375000010319 |
| | 300 | 0.34505907515618 | 0.34374990531351 | 0.34375000010319 |
| $y = 0$ | 50 | -0.12500287386101 | -0.1250000777502 | -0.1249999302999 |
| | 100 | -0.12500285981042 | -0.12500000000094 | -0.12500000000001 |
| | 200 | -0.12500285981040 | -0.12500000000095 | -0.12500000000000 |
| | 300 | -0.12500285981040 | -0.12500000000095 | -0.12500000000000 |
| $y = -A/2$ | 50 | -0.40754876310628 | -0.40624844239106 | -0.40625144451786 |
| | 100 | -0.40755695832287 | -0.40624990925386 | -0.40625000362014 |
| | 200 | -0.40755695075362 | -0.40624990531291 | -0.40625000010320 |
| | 300 | -0.40755695075362 | -0.40624990531291 | -0.40625000010320 |
| $y = -A$ | 50 | 1.014 | 1.007 | 0.993 |
| | 100 | 0.992 | 0.996 | 0.996 |
| | 200 | 0.9964 | 0.9982 | 0.9984 |
| $S = -1.0$ and $A = 1.0$ | | | | |
| y | n | actual values of ψ | | |
| | | $x = -0.7$ | $x = -0.3$ | $x = 0.0$ |
| $y = 1.0$ | 10 | -1.068 | -1.035 | -0.968 |
| | 20 | -0.965 | -0.982 | -0.984 |
| | 50 | -1.014 | -1.007 | -0.993 |
| | 100 | -0.992 | -0.996 | -0.996 |
| $y = 0.5$ | 10 | -0.069175427893891 | -0.27044200038033 | -0.32634509494049 |
| | 20 | -0.069175472292034 | -0.27044205430477 | -0.32634504155722 |
| | 50 | -0.069175472292028 | -0.27044205430476 | -0.32634504155721 |
| | 100 | -0.069175472292028 | -0.27044205430476 | -0.32634504155721 |
| $y = -0.5$ | 10 | 0.069175427893891 | 0.27044200038033 | 0.32634509494049 |
| | 20 | 0.069175472292034 | 0.27044205430477 | 0.32634504155722 |
| | 50 | 0.069175472292028 | 0.27044205430476 | 0.32634504155721 |
| | 100 | 0.069175472292028 | 0.27044205430476 | 0.32634504155721 |
| $y = -0.5$ | 10 | 1.068 | 1.035 | 0.968 |
| | 20 | 0.965 | 0.982 | 0.984 |
| | 50 | 1.014 | 1.007 | 0.993 |
| | 100 | 0.992 | 0.996 | 0.996 |

References

- [1] R.C.T. Smith, "The Bending of a Semi-Infinite Strip", Austral. J. Sci. Res., 5, 227-237 (1952).
- [2] D.D. Joseph and L. Sturges, "The Free Surface on a Liquid Filling a Trench Heated from Its Side", J. Fluid Mech., 69, 565-589 (1975).
- [3] D.D. Joseph, "The Convergence of Biorthogonal Series For Biharmonic and Stokes Flow Edge Problems: Part I", S.I.A.M. J. Appl. Math., 33, 337-347 (1977).
- [4] D.D. Joseph and L. Sturges, "The Convergence of Biorthogonal Series For Biharmonic and Stokes Flow Edge Problems: Part II", SIAM. J. Appl. Math., 34, 7-27 (1978).
- [5] F. Gürçan, "PhD Thesis", University of Leeds, (1997).

- [6] P.N. Shankar, "The Eddy Structure in Stokes Flow in a Cavity", *Fluid Mech.*, 250, 371-383 (1993).
- [7] P.H. Gaskell, M.D. Savage, J.L. Summers and H.M. Thompson, "Modeling and Analysis of Meniscus Roll Coating", *J. Fluids Mech.*, 298, 113-137 (1995).
- [8] P.H. Gaskell, F. Gürçan, M.D. Savage and H.M. Thompson, "Stokes Flow in Closed, Rectangular Domain", *Proc. IMCHEME J of Eng. Sci. Part C*, 212, 5, 387-403 (1998).
- [9] P.H. Gaskell, M.D. Savage, J.L. Summers and H.M. Thompson, "Creeping Flow Analyses of Free Surface Cavity Flows", *Theo. Comp. Fluids Dynam.*, 8, 415-433 (1996).
- [10] H.K. Moffatt, "Viscous and Resistive Eddies Near a Sharp Corner", *Fluid Mech.*, 18, 1-18 (1964).
- [11] C.K. Aidun, N.G. Triantafillopoulos and J.D. Benson, "Numerical Study of Viscous Flow in a Cavity", *Phys. Fluids (A)*, 3, 2081-2091 (1991).
- [12] J.M. Floryan and L. Czechowski, "On the Numerical Treatment of Corner Singularity in the Vorticity Field", *J. Comput. Phys.*, 118, 222-228 (1995).
- [13] M.A. Kelmanson, "Modified Integral Equation Solution of Viscous Flow near Sharp Corners", *Computer and Fluids*, 11, 307-318 (1983).
- [14] G.K. Batchelor, "An Introduction to Fluid Dynamics", Cambridge University Press, Cambridge, England, (1967).